Limnol. Oceanogr., 54(4), 2009, 1243–1256

Effect of fully characterized unsteady flow on population growth of the dinoflagellate *Lingulodinium polyedrum*

Michael I. Latz,[a,*] Jeffrey Allen,[b] Sutanu Sarkar,[c] and Jim Rohr[a,b]

[a] Scripps Institution of Oceanography, University of California San Diego, La Jolla, California
[b] Space and Warfare Systems Center Pacific at San Diego, San Diego, California
[c] Department of Mechanical and Aerospace Engineering, University of California San Diego, La Jolla, California

Abstract

Dinoflagellate population growth is inhibited by fluid motion, which is typically characterized by some average flow property, regardless if the flow is steady or unsteady. This study compares the effect of fully characterized steady and unsteady flow on net population growth of the red tide dinoflagellate *Lingulodinium polyedrum*. The unsteady flow fields were generated using oscillatory laminar Couette flow and characterized analytically to provide complete knowledge of the fluid shear exposure over space and time throughout the chamber. Experimental conditions were selected so all cells experienced a similar shear exposure regardless of their position within the chamber. Unsteady flow with maximum shears of 6.4 s^{-1} and 6.7 s^{-1} and an average absolute shear of 4 s^{-1}, comparable with levels found at the ocean surface on a windy day, resulted in higher levels of growth inhibition than for steady Couette flow with shears of 4 and 8 s^{-1}. Over the parameter space studied, growth inhibition increased with increasing treatment duration (5–120 min) but was insensitive to oscillation period (60–600 s) or whether the unsteady flow changed in direction. These results indicate that over the parameter space studied, unsteady flow is more inhibitory to net growth than steady flow, for the same average flow conditions, and demonstrate that flow characterization on the basis only of average flow properties is inadequate for comparing population growth in unsteady and steady flows.

All plankton experience unsteady fluid motion because of wind, waves, tides, and currents (Margalef 1997). Turbulence promotes water-column mixing, affecting the amount of stratification, increasing vertical mixing and decreasing the average light field for photosynthetic organisms, and affecting the distribution of nutrients (Kiørboe 1993; Smayda 2000; Smayda and Reynolds 2001). Conceptual models such as Margalef's Mandela (Margalef et al. 1979) attest to the importance of turbulence in regulating the population dynamics of phytoplankton (Smayda and Reynolds 2001), with dinoflagellates generally favoring conditions of low turbulence. Field data show a negative correlation between dinoflagellate abundance and flow agitation levels associated with wind, waves, and turbulence conditions (Pollingher and Zemel 1981; Berman and Shteinman 1998; Stoecker et al. 2006), and dinoflagellates can accumulate in depth strata with low turbulence (Sullivan et al. 2003), although they can concentrate at frontal zones, which can be regions of enhanced turbulence (Smayda 2000). Dinoflagellate red tides are commonly associated with periods of calm water (Allen 1946; Margalef et al. 1979; Smayda and Reynolds 2001). Most laboratory studies report that the population growth of dinoflagellate species decreases when cells are agitated by shaking, aeration, or stirring (White 1976; Pollingher and Zemel 1981; Berdalet et al. 2007), although flow can in some cases have no effect on population growth or even promote growth (Sullivan and Swift 2003; Sullivan et al. 2003). Of fundamental importance is establishing a robust experimental approach for investigating the hydrodynamic interaction of turbulence with individual cells to determine cellular mechanisms involved in flow responses.

Turbulent experimental flow fields have been widely used to compare the effect of high- and low-turbulence treatments on the growth of dinoflagellates (Sullivan and Swift 2003; Havskum et al. 2005; Bolli et al. 2007), ciliates (Dolan et al. 2003), and bacteria (Peters et al. 2002; Malits et al. 2004). A popular experimental approach to study the effect of oceanic turbulence on population growth has been to use turbulent flows created by moving a grid or rods through the test tank, or by shaking flasks. These approaches are considered to most closely emulate oceanic flow, and they allow different turbulence levels to be generated (Peters and Redondo 1997). In these growth studies, the turbulent flow is characterized by a single averaged parameter measured for only a part of the flow volume and agitation cycle (Alcaraz et al. 1988; Peters and Gross 1994; Sullivan and Swift 2003). However, the energy dissipation associated with grid turbulence decreases rapidly in time (t), roughly as $1/t^2$ (Hinze 1975) after the grid passes, and in distance (x) behind the grid, roughly as $1/x^2$ (Tennekes and Lumley 1972), and also may depend on the grid spacing and dimensions. Consequently, it is not surprising that turbulence studies have reported order-of-magnitude or more spatial and temporal variability in energy dissipation or shear within a flow treatment (Peters and Gross 1994; Sullivan and Swift 2003; Berdalet et al. 2007), spatial heterogeneity in organism distribution within the test volume (Bolli et al. 2007), and dramatically different effects on growth of the same species, ranging from enhancement to inhibition (Sullivan and Swift 2003; Havskum et al. 2005).

At the small spatial scales of phytoplankton, turbulent velocity fluctuations are experienced as laminar flow with

*Corresponding author: mlatz@ucsd.edu

unsteady rates of strain (i.e., shear) (Lazier and Mann 1989; Thomas and Gibson 1990*a*,*b*). One experimental approach to investigate the effect of fluid shear on dinoflagellate growth is simple laminar Couette flow generated in the gap between concentric cylinders with only the outer cylinder rotating at a constant rate. The advantage of laminar Couette flow is that the flow field is fully characterized on the basis of the dimensions of the cylinders and the angular rotation of the outer cylinder (Taylor 1923; Van Duuren 1968); for steady rotation of the outer cylinder the shear level in the gap is nearly uniform so that all organisms experience a similar flow field with nearly constant levels of fluid rate of strain (i.e., shear rate). Steady Couette flow has been used to study the effect of fluid shear on the population growth of *Lingulodinium polyedrum* (Thomas and Gibson 1990*b*; Juhl et al. 2000; Juhl and Latz 2002) and other dinoflagellates (Juhl et al. 2001; Stoecker et al. 2006). The reported shear rate threshold for growth inhibition for *L. polyedrum* is approximately 2 s^{-1} (Thomas and Gibson 1990*a*), equivalent to a rate of dissipation of kinetic energy per unit mass, ε, of the order of 10^{-6} m^2 s^{-3} (Rohr et al. 2002). These values of ε are present in the upper ocean under conditions of wind and wave forcing (Mackenzie and Leggett 1993; Smyth and Moum 2001), where waves breaking at the ocean surface create a layer of enhanced dissipation (Anis and Moum 1995; Drennan et al. 1996; Veron and Melville 1999). Thus, experimental results using steady laminar shear flow support field observations that dissipation rate levels present in surface waters on a windy day may inhibit dinoflagellate population growth (Thomas and Gibson 1990*a*; Berman and Shteinman 1998). However, an obvious limitation of using steady laminar flow is that it cannot fully emulate the inherently unsteady flow environment in the ocean.

The objective of the present study was to test the effect of unsteady flow on dinoflagellate population growth, using an experimental approach in which the unsteady flow field was fully characterized. Furthermore, by using the same growth chambers as in previous studies testing steady laminar flow, the effect of unsteady and steady flows can be directly compared. The use of oscillatory laminar Couette flow within a prescribed parameter space provides access to an analytical framework, which with a few reasonable assumptions results in complete knowledge of the unsteady flow field. The dinoflagellate *L. polyedrum*, known as a source of red tides during calm conditions (Allen 1946; Sweeney 1975; Harrison 1976) and considered a representative species for studying the effect of turbulence on dinoflagellate population growth (Smayda 2000; Smayda and Reynolds 2001), was chosen because the effect of laminar fluid shear on its population growth is well documented for steady flow (Thomas and Gibson 1990*b*; Juhl et al. 2000; Juhl and Latz 2002). Furthermore, we can characterize its population growth in a fully characterized unsteady flow field using the identical apparatus and growth conditions as was previously used in studies with steady flow (Juhl et al. 2000; Juhl and Latz 2002). In using the identical apparatus the smallest oscillation period is limited to about 60 s, as shorter periods result in flow conditions with unacceptable spatial dependence in shear history; consequently the timescales of the unsteady Couette flow were much larger than those typical of turbulence behind a grid or associated with ocean turbulence. Nevertheless, the present investigation is designed as a first step toward studying the effect of steady and unsteady shear flows on dinoflagellate growth in a series of fully characterized flow conditions. A similar approach of using the same apparatus to compare the effect of steady and unsteady laminar flows has been used in studies with mammalian cells (Dardik et al. 2005; Yee et al. 2008). Notably, it has been found that the response of endothelial cells is more sensitive to unsteady than steady flows (Barakat and Lieu 2003).

This study consisted of 25 growth experiments, each 10 d in duration and containing four replicate flow chambers and four replicate still control chambers. Population growth of *L. polyedrum* was measured in steady flows with constant levels of shear rate ranging from 1.8 to 8 s^{-1} and unsteady, oscillatory flows with average absolute shear rates ranging from 1.8 to 4 s^{-1}. Tests investigated the effect of average absolute shear level, duration, period of oscillation, and changing flow direction on population growth in unsteady flow. For the parameter space studied, this initial study demonstrates that unsteady flows resulted in greater growth inhibition than steady flows with the same average flow properties.

Methods

Experimental organisms—All experiments used the identical nonaxenic, unialgal strain of *L. polyedrum* (Stein) Dodge 1989 (formerly *Gonyaulax polyedra*) whose shear sensitivity has been extensively characterized in steady flow using similar experimental methods (Thomas and Gibson 1990*a*; Juhl et al. 2000; Juhl and Latz 2002) as those used in this study. One to two days before each experiment, *L. polyedrum* cells were inoculated into fresh f/4 medium minus silicate (Guillard and Ryther 1962) at an approximate concentration of 500 cells mL^{-1} and maintained at a temperature of 21°C on a 12 : 12 h light : dark cycle. Illumination level for all experiments was approximately 30 μmol quanta m^{-2} s^{-1}, provided by two 40-W cool-white fluorescent bulbs located 20 cm above the top of the chambers.

Pairs of experiments were conducted simultaneously, and consisted of 12 chambers divided into three groups: four replicate chambers were used as still controls, four were exposed to one flow condition, and four were exposed to a different flow condition. Thus, every flow treatment had a simultaneous still control condition. This paired experimental design accounted for temporal variation in the growth rates of cultures due to changes in illumination or other factors independent of the flow history of the cells.

On day zero, each flow chamber was loaded with 170 mL of culture. For an initial period of 3 d, all chambers remained still to verify positive net growth; in a few experiments a chamber not satisfying this criterion was discarded. Thereafter, each chamber was randomly assigned as a control or to one of two shear treatments. Unless otherwise stated, during the treatment period daily

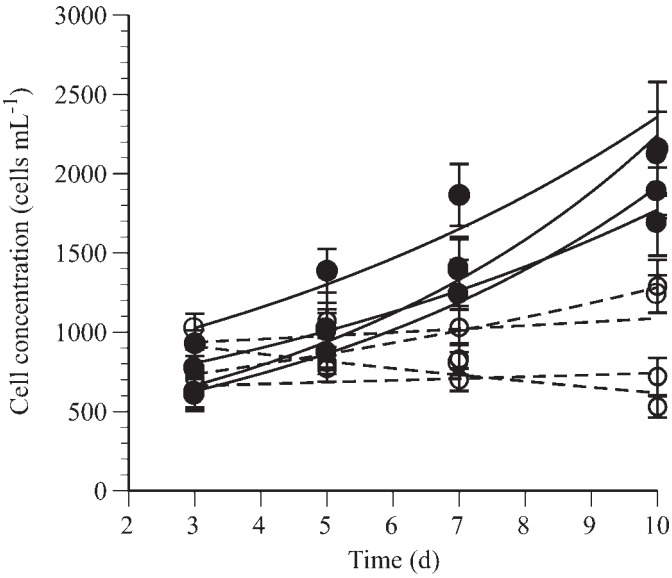

Fig. 1. Representative experiment (expt. O4) showing the effect of flow treatment on net population growth of *Lingulodinium polyedrum*. Symbols represent the average ± SE cell concentration from five subsamples. Chambers were inoculated at day 0 and remained still during an initial period; at day 3 half the chambers (open symbols) were exposed to 2 h d^{-1} of oscillatory flow having a period of 100 s and average absolute shear of 4 s^{-1}, while the other half (solid symbols) remained still as controls. Curves represent the least-squares exponential regressions of cell concentration vs. time, where the slope is the net growth rate. The slopes for each treatment were averaged to obtain results shown in Table 1.

shear exposure was 2 h, a duration sufficient to cause maximum growth inhibition for steady shear levels above the response threshold (Juhl and Latz 2002). The shear treatment started 2 h before the end of the night phase when cells are most shear sensitive (Juhl et al. 2000), while adjacent control chambers always remained still. The position of each group of four replicate chambers was randomly changed every 2–3 d, after cell counting, to avoid biases in growth rate due to any positional variation in illumination.

Cultures in the still control group remained in exponential growth phase during the entire 10-d duration of the experiment. For determining cell concentrations during the steady and unsteady shear experiments, triplicate 0.5-mL samples from each chamber were sampled every 2–3 d during the middle of the light phase, when cell division does not occur and cultures are the least shear sensitive (Juhl et al. 2000). After gentle mixing, the pooled samples were subsampled as five replicate volumes of 10–25 μL for cell counting. The exponential net population growth rate, μ, was calculated for each replicate still and sheared chamber from the change in cell concentration over the 7-d treatment period on the basis of the least-squares linear regression of the natural logarithm of cell concentration vs. time (Fig. 1). Means and standard deviations of population growth rates were calculated from values obtained from four replicate chambers for each condition in an experiment.

Percentage growth inhibition for each individual sheared chamber was calculated as the relative change in its growth rate from the average of the corresponding controls (Juhl et al. 2000):

$$\% \text{ growth inhibition} = \frac{\overline{\mu}_{\text{control}} - \mu_{\text{sheared}}}{\overline{\mu}_{\text{control}}} \times 100 \quad (1)$$

Growth inhibition of 0% signifies identical growth rates of sheared cultures to still controls, a value of 100% indicates no net growth occurred for the sheared cultures, values >100% reflect a decrease in the population for the sheared cultures due to mortality (Juhl and Latz 2002), and negative values, although never observed, would indicate greater growth rates in the sheared cultures compared with the controls. Because proportional (percentage) data tend to form a binomial rather than normal distribution (Zar 1974), data were arcsine square-root transformed before statistical analysis (Juhl and Latz 2002) unless an experiment had negative growth rates, in which data could not be transformed and the untransformed data were analyzed. Trends of significance were not altered by the use of untransformed data for statistical analyses. Values of percentage growth inhibition were expressed as means with standard deviation of the mean, with n equaling the number of replicate sheared chambers per treatment. Significant differences were tested using unpaired t-tests, one-way ANOVA, or least-squares linear regressions between variables with significance on the basis of the $p = 0.05$ level. All statistical analyses were performed using Statview software (SAS Institute).

Analytical methods—The Couette flow chambers were identical to those used by Juhl et al. (2001) and consisted of concentric cylinders constructed of clear acrylic, with inner and outer cylinder radii of 4.1 and 4.8 cm, respectively, and a chamber height of 20 cm. The bottom of the inner cylinder was in contact with the base of the chamber so there was no "dead" volume within the apparatus. To minimize flow instabilities, the ratio of gap width to outer cylinder radius was <0.2 (Van Duuren 1968). Flow visualization tests using 2.5% AQ-1000 Kalliroscope Rheoscope concentrate (Kalliroscope Corp.) in filtered seawater confirmed that the flow was always laminar and secondary flows were not present.

Because of the relatively narrow gap width, h, between the cylinders, the velocity field was modeled as Couette flow, the laminar flow between infinite parallel plates with the outer plate moving, either steady or oscillatory, and the inner plate stationary (Fig. 2). For the inner and outer cylinder radii, the parallel-plate approximation will predict shear stresses within 10% of the correct value (Fox et al. 2004). The velocity $u(t,y)$ depends only on time t and position y above the lower plate; it is governed by the diffusion equation with kinematic viscosity v (Schlichting 1979),

$$u_t = v u_{yy} \quad (2)$$

The boundary conditions depend on the particular flow required. For all flows the lower plate is stationary,

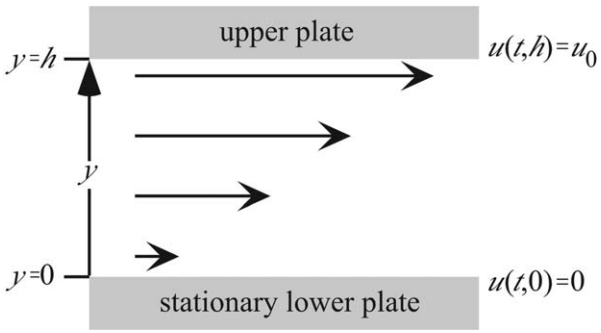

Fig. 2. Flat-plate approximation to the fluid flow between the stationary inner cylinder and the moving upper cylinder. The radial coordinate starts at $y = 0$ from the stationary plate and increases to $y = h$ at the upper plate. Fluid flow is parallel between the plates so the speed $u(t,y)$ depends only on the time t and the radial coordinate y.

$$u(t,0) = 0 \tag{3}$$

For still controls the upper plate is also stationary,

$$u(t,h) = 0 \tag{4}$$

For steady flow the the upper plate moves at constant speed,

$$u(t,h) = u_0 \tag{5}$$

and the flow field is characterized by nearly constant shear across the gap (Van Duuren 1968; Schlichting 1979). For oscillatory flow the upper plate moves sinusoidally,

$$u(t,h) = u_0 \cos(\omega t) \tag{6}$$

where ω is the angular velocity ($\omega = 2\pi N/60$, where N is the rotational speed in revolutions per minute [rpm]). For rectified oscillatory flow the upper plate moves sinusoidally but always in the same direction,

$$u(t,h) = u_0 |\cos(\omega t)| \tag{7}$$

The response of the fluid, initially at rest, to the oscillatory wall motion is an initial transient that settles into a harmonic oscillation with angular frequency ω and different phase throughout the gap. Only the steady-state, harmonic oscillatory response is considered because the transient response is essentially over within a period (Panton 1968). The complex solution for this oscillation is

$$u(t,y) = u_0 \frac{\sinh(\beta y)}{\sinh(\beta h)} \exp(i\omega t) \tag{8}$$

where $\beta = (\omega/\nu)^{1/2} \exp(i\pi/4)$. The quantity $[\nu/\omega]^{1/2}$ is proportional to the depth of penetration of the oscillatory flow (Schlichting 1979). The fluid rate of strain, hereafter simply referred to as shear, is the real part of Eq. 8, $\mathrm{Re}[u_y(t,y)]$. The average absolute value of mean shear was calculated as $(hT)^{-1} \int_0^T \int_0^h |\mathrm{Re}[u_y(t,y)]| \mathrm{d}y\mathrm{d}t$ and the average kinetic energy dissipation per unit mass, ε, was calculated as $\nu(/hT)^{-1} \int_0^T \int_0^h \mathrm{Re}[u_y(t,y)]^2 \mathrm{d}y\mathrm{d}t$. Numerical simulations showed that for the experimental geometry chosen, oscillation periods <60 s resulted in unacceptable spatial dependence in shear history within the chamber.

Experimental methods—The rotation of the outer cylinder was controlled by a Silvermax servomotor (Quicksilver Controls) coupled to a 6:1 gearbox and pulley system using plastic chain so that four replicate chambers are driven by one servomotor. Servomotor velocity was controlled by custom software on a personal computer, with user control of the outer cylinder speed, which is constant for steady flow treatments and varies sinusoidally for unsteady flow treatments. In both cases, the starting and ending times for the daily flow treatments were specified in the software to allow unattended operation. Experimental design was optimized to address the following null hypothesis: Unsteady and steady flows with the same average absolute shear cause similar amounts of growth inhibition.

The effect of unsteady flow produced by sinusoidal oscillation of the outer cylinder on net population growth was compared with that of steady flow with the identical average absolute shear value of 1.8, 3, or 4 s^{-1}. A steady shear level of 4 s^{-1}, equivalent to an average rate of kinetic energy dissipation, ε, of 2×10^{-5} m^2 s^{-3}, is known to inhibit growth of *L. polyedrum* under steady flow conditions (Thomas and Gibson 1990*a*,*b*; Juhl and Latz 2002), and occurs in near-surface waters during moderate winds (Thomas and Gibson 1990*b*; Brainerd and Gregg 1993). The maximum shear for the oscillatory case increased as a function of decreasing period of oscillation. For an absolute average shear of 4 s^{-1}, maximum shear ranged between 6.4 and 11.3 s^{-1} as the period decreased from 600 to 60 rpm (Table 1). Unsteady flows with periods >100 s always had shear levels less than that for the steady case of 8 s^{-1} In addition, the effect of unsteady flow with a maximum shear of 4 s^{-1} was compared with that for steady flow with an average shear of 4 s^{-1}. Finally, steady flow treatments were compared with previous studies using the identical strain of *L. polyedrum* (Juhl et al. 2000; Juhl and Latz 2002).

Sinusoidal forcing of the outer cylinder exposed the cells to a flow field that was alternately changing directions. To investigate the possible effect of changing flow direction on population growth, cells were also exposed to both steady and rectified sinusoidal laminar flow with nearly identical average absolute shear levels. For the rectified case the outer cylinder always rotated in one direction with a minimum rpm of zero, with an identical average absolute shear but without flow reversal.

Finally, a series of unsteady flow experiments with constant period and absolute average shear investigated the effect of flow duration to compare with previous steady flow experiments, where growth inhibition increases with increasing flow duration (Juhl and Latz 2002). The parameter space for unsteady flow treatments was constrained by the requirement to minimize spatial gradients in shear within the flow volume while using the identical apparatus as previous studies working with

Table 1. Summary of results of growth experiments on the effect of steady flow and unsteady oscillatory flow treatments on the net population growth of *Lingulodinium polyedrum*. u_0 is the rotation rate for steady flow and maximum rotation rate for oscillatory flow. *See* text for details on experimental and analysis methods. Net population growth rate (μ) and percentage growth inhibition are expressed as mean ± SD, with number of replicate chambers per treatment in parentheses.

Experiment	u_0 (rpm)	Period (s)	Duration (h d^{-1})	Average absolute shear (s^{-1})	Maximum shear (s^{-1})	Root mean square shear (s^{-1})	Dissipation rate (m^2 s^{-3})	Net growth, μ (d^{-1})		% growth inhibition
								Control	Sheared	
Steady flow										
S1	4.50	–	2	3.0	3.0	–	9.0×10^{-6}	0.189 ± 0.014 (3)	0.120 ± 0.030 (4)	36.4 ± 15.7
S2	6.00	–	2	4.0	4.0	–	1.6×10^{-5}	0.146 ± 0.014 (3)	0.082 ± 0.045 (4)	43.7 ± 31.1
S3	6.00	–	2	4.0	4.0	–	1.6×10^{-5}	0.123 ± 0.008 (3)	0.061 ± 0.031 (3)	50.2 ± 25.4
S4	12.00	–	2	8.0	8.0	–	6.4×10^{-5}	0.100 ± 0.031 (3)	0.031 ± 0.039 (4)	69.2 ± 39.1
S5	2.72	–	2	1.8	1.8	–	3.2×10^{-6}	0.131 ± 0.013 (4)	0.064 ± 0.035 (4)	51.4 ± 26.5
S6	2.72	–	2	1.8	1.8	–	3.2×10^{-6}	0.151 ± 0.046 (4)	0.078 ± 0.027 (4)	48.2 ± 18.0
S7	2.72	–	2	1.8	1.8	–	3.2×10^{-6}	0.113 ± 0.020 (4)	0.078 ± 0.034 (4)	31.4 ± 29.9
Oscillatory flow										
O1	7.53	60	2	4.0	11.3	4.6	2.1×10^{-5}	0.139 ± 0.010 (4)	−0.010 ± 0.043 (4)	107.2 ± 31.1
O2	8.10	100	2	4.0	8.9	4.5	2.0×10^{-5}	0.155 ± 0.022 (3)	0.019 ± 0.068 (4)	87.7 ± 44.1
O3	8.10	100	2	4.0	8.9	4.5	2.0×10^{-5}	0.126 ± 0.024 (4)	0.014 ± 0.035 (4)	89.3 ± 27.3
O4	8.10	100	2	4.0	8.9	4.5	2.0×10^{-5}	0.141 ± 0.030 (4)	0.015 ± 0.056 (4)	89.1 ± 39.4
O5	8.65	300	2	4.0	6.7	4.4	1.9×10^{-5}	0.139 ± 0.010 (4)	−0.001 ± 0.064 (4)	100.6 ± 46.0
O6	8.72	600	2	4.0	6.4	4.4	1.9×10^{-5}	0.126 ± 0.024 (4)	−0.004 ± 0.064 (4)	103.5 ± 50.4
O7	3.65	100	2	1.8	4.0	2.0	4.0×10^{-6}	0.131 ± 0.013 (4)	0.069 ± 0.042 (4)	47.3 ± 31.9
O8	3.65	100	2	1.8	4.0	2.0	4.0×10^{-6}	0.107 ± 0.024 (4)	0.057 ± 0.004 (3)	46.5 ± 3.5
O9	3.65	100	2	1.8	4.0	2.0	4.0×10^{-6}	0.151 ± 0.046 (4)	0.088 ± 0.021 (4)	42.0 ± 14.0
O10	8.10	100	1	4.0	8.9	4.5	2.0×10^{-5}	0.141 ± 0.030 (4)	0.065 ± 0.037 (4)	54.1 ± 26.4
O11	8.10	100	0.75	4.0	8.9	4.5	2.0×10^{-5}	0.101 ± 0.030 (4)	0.037 ± 0.040 (4)	63.6 ± 40.9
O12	8.10	100	0.5	4.0	8.9	4.5	2.0×10^{-5}	0.125 ± 0.020 (4)	0.055 ± 0.040 (4)	55.8 ± 30.2
O13	8.10	100	0.25	4.0	8.9	4.5	2.0×10^{-5}	0.125 ± 0.020 (4)	0.097 ± 0.040 (4)	22.4 ± 21.0
O14	8.10	100	0.083	4.0	8.9	4.5	2.0×10^{-5}	0.101 ± 0.030 (4)	0.090 ± 0.040 (4)	11.4 ± 37.3
Rectified oscillatory flow comparison										
Rectified15	6.70	300	2	3.1	5.2	3.4	1.2×10^{-5}	0.146 ± 0.045 (4)	0.059 ± 0.049 (4)	59.6 ± 33.3
O15	6.70	300	2	3.1	5.2	3.4	1.2×10^{-5}	0.146 ± 0.045 (4)	0.061 ± 0.028 (4)	58.4 ± 19.0
Rectified16	8.67	300	2	4.0	6.7	4.4	1.9×10^{-5}	0.168 ± 0.027 (4)	0.050 ± 0.035 (4)	70.4 ± 20.7
O16	8.67	300	2	4.0	6.7	4.4	1.9×10^{-5}	0.168 ± 0.027 (4)	0.039 ± 0.038 (4)	76.9 ± 22.8

steady flow conditions (Juhl et al. 2000; Juhl and Latz 2002).

Results

Description of the unsteady flow field—The oscillation amplitude and frequency of the rotation of the outer cylinder (Fig. 3A) was optimized to provide the desired average absolute shear while minimizing spatial variability in shear levels within the gap, so that all cells in the chamber experienced similar shear histories, regardless of position (Fig. 3B). The associated frequency distribution of shear values, referred to as the probability density function, was calculated for each experiment to give expected values of shear in space and time (Fig. 3C). According to sine wave properties, oscillatory flow treatments were expected to produce maximum shear levels about 1.6 times greater than the average absolute shear. At the lower frequencies studied, periods of 300 and 600 s, this relation was approximately achieved within the test chambers. But at higher frequencies, periods of 60 and 100 s, the maximum amplitude was about 2.8 and 2.2 times the average absolute value. Although cells exposed to unsteady flow experienced both lower and higher levels of shear than the average, the entire range of shear values in the gap was always fully characterized, allowing calculation of absolute value of average and maximum shear, the shear probability density function, and average kinetic energy dissipation per unit mass within the test chamber (Table 1).

Average absolute shear for steady vs. unsteady flows—Net population growth rate for the pooled still controls was 0.14 ± 0.03 d^{-1} (expts. S1–S7, O1–O16, R15, 16, $n = 57$ replicate chambers, Table 1), similar to that of Juhl et al. (2000) and Juhl and Latz (2002) working with the identical strain of *L. polyedrum* and using similar growth conditions. Steady flow treatment for 2 h d^{-1} with a shear of 4 s^{-1} (expts. S2, S3) resulted in positive net growth but with $46.5\% \pm 26.7\%$ growth inhibition compared with the still controls. Oscillatory unsteady flow treatment for the same daily duration and average absolute shear of 4 s^{-1} resulted in almost complete inhibition of population growth. For example, treatment with a period of 100 s (expts. O2–O4) resulted in $88.7\% \pm 34.0\%$ growth inhibition. Including all oscillation periods (60–300 s) with an average absolute shear of 4 s^{-1} and 2 h d^{-1} duration (expts. O1–O6, O16), overall growth inhibition for unsteady flow was $93.5\% \pm 35.4\%$. Thus for the same average absolute shear of 4 s^{-1}, unsteady flows (expts. O1–O6, O16) resulted in growth inhibition that was 50% greater and significantly different (t-test, $t = 2.588$, df = 34, $p = 0.014$) than for steady flow (expts. S2, S3). When similar experiments were repeated for a slightly lower absolute average shear of 3 s^{-1}, growth inhibition for the unsteady flow treatment (expt. O15) was 38% higher than for the steady flow treatment (expt. S1), although the difference was not significantly different (t-test, $t = 1.808$, df = 6, $p = 0.121$). For an even lower absolute average shear of 1.8 s^{-1}, growth inhibition of $45\% \pm 3\%$ for unsteady flow (expts. O7–O9) was similar (t-test, $t = 0.002$, df = 21, $p = 0.999$) to the growth inhibition of $43\% \pm 10\%$ for steady flow (expts. S5–S7). Thus as the shear level decreases, the difference in growth inhibition diminishes between unsteady and steady flow treatments with similar average absolute shear levels.

Remarkably, growth inhibition for a steady flow treatment with a shear of 8 s^{-1} (expt. S4) was not significantly different (t-test, $t = 1.073$, df = 14, $p = 0.301$) from that for unsteady treatments with an average absolute shear of 4 s^{-1} and maximum shear values of 6.4 (expts. O6) and 6.7 s^{-1} (expts. O5, O16), even though the shear level for the steady treatment was always higher than the maximum levels for the unsteady treatments. These experiments show that the amount of growth inhibition is not due solely to the average level of shear, but is also dependent on whether the shear flow was steady or unsteady (Fig. 4).

Effect of oscillation period, changing flow direction, and shear treatment duration—For unsteady flow with an average absolute shear of 4 s^{-1} and 2 h d^{-1} shear duration, there was no apparent effect of oscillation period for the 60–600-s range tested (Table 1); the slope of the linear regression of growth inhibition as a function of oscillation period was not significantly different from zero (exps. O1–O6; t-test, $t = -0.110$, df = 22, $p = 0.913$, $R^2 = 0.001$). Under these conditions growth was nearly always completely inhibited; the effect of oscillation period at different average absolute shears and different durations is not known.

In oscillatory flow, the flow direction reverses during each oscillation period (Fig. 3A). Two pairs of experiments (expts. R15, O15 and R16, O16) addressed whether the change in flow direction affected growth inhibition. The effect of oscillatory flow was compared with that of rectified oscillatory flow in which flow direction was not reversed but otherwise the flow conditions were nearly identical. For experiments using a 300-s period and an average absolute shear of 4.0 s^{-1} with maximum shear of 6.7 s^{-1}, there was no significant difference in growth inhibition between oscillatory and rectified oscillatory flow (expts. R16, O16; t-test, $t = 0.422$, df = 6, $p = 0.688$). A similar result occurred for experiments with oscillatory and rectified oscillatory flows having an average absolute shear of 3.1 s^{-1} with maximum shear of 5.2 s^{-1} (expts. R15, O15; t-test, $t = -0.058$, df = 6, $p = 0.956$). Thus unsteady flow treatments with identical absolute shear levels resulted in similar amounts of growth inhibition, regardless of whether the flow direction reversed. As expected, the unsteady treatment having an average absolute shear of 3.1 s^{-1} resulted in 24% less growth inhibition than the unsteady 4 s^{-1} treatment, although due to experimental variability the results were not statistically different (t-test, $t = 1.238$, df = 6, $p = 0.262$).

The effect of the duration of unsteady flow was examined for an average absolute shear of 4 s^{-1}, period of 100 s, and daily durations of 5 min to 2 h (expts. O10–O14; Table 1; Fig. 5). All flow exposures resulted in growth inhibition, with the minimum exposure of 5 min resulting in 11% growth inhibition. The amount of growth inhibition increased with increasing flow duration. For steady flow

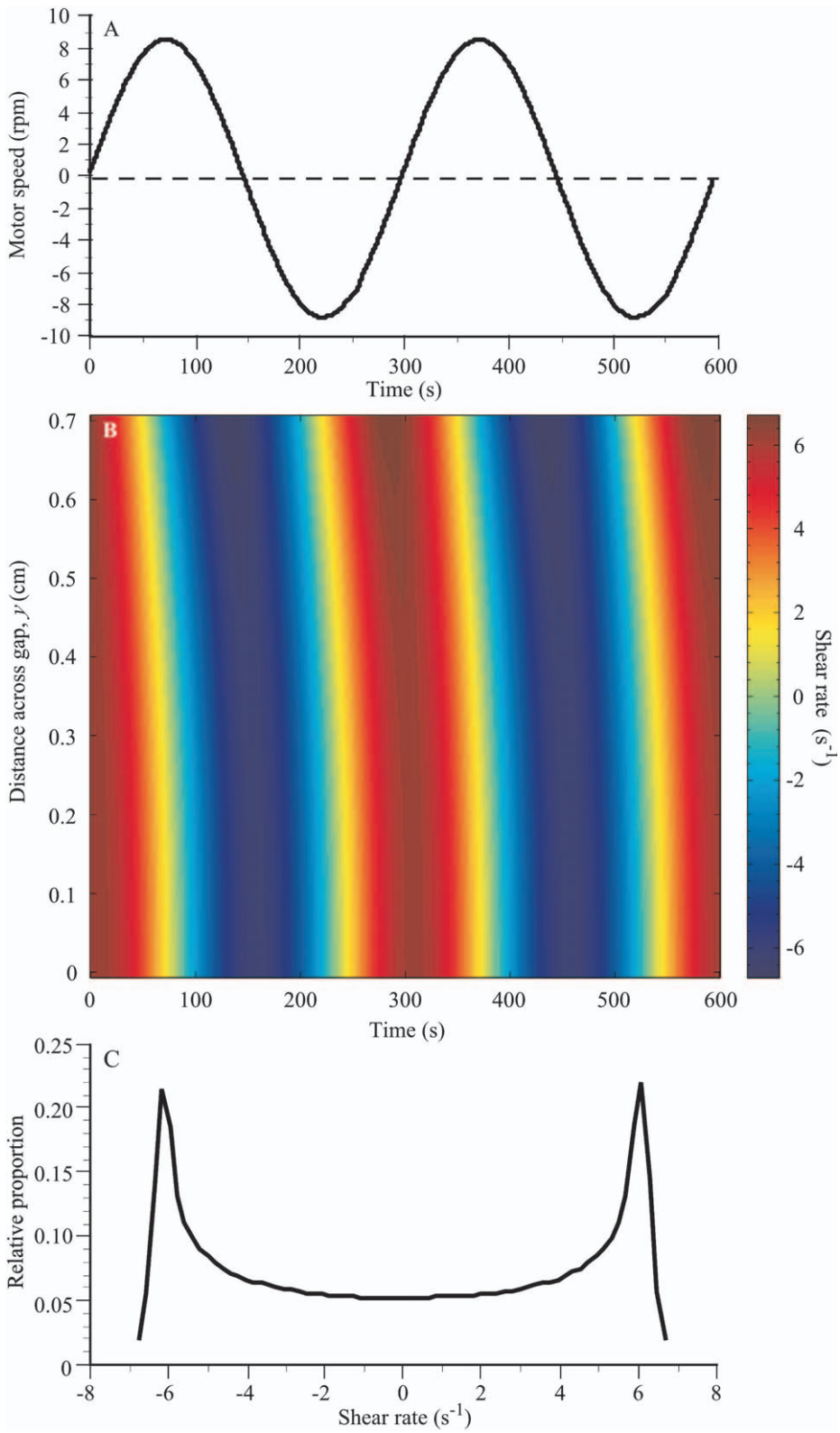

Fig. 3. Oscillatory Couette flow for a 300-s oscillation period and average absolute shear of 4 s^{-1} (expt. O4). (A) Motor rpm forcing rotation of the outer Couette cylinder as a function of time, shown for two periods of rotation. The rpm value follows a sine function with reversal of the outer cylinder and flow direction. (B) Representative spatial and temporal distribution of fluid shear, $u_y(t,y)$, for the steady-state oscillatory flow field within the gap between cylinders, shown for two periods of rotation. The origin is at the wall of the inner cylinder and 0.7 cm refers to the wall of the outer (rotating) cylinder. There were minimal spatial gradients of shear across the gap. (C) Probability density function of shear within the gap for one cycle of unsteady oscillatory flow. The distribution was ''saddle'' shaped with minimum probability at a shear of 0 s^{-1} and modes at -6 and 6 s^{-1}.

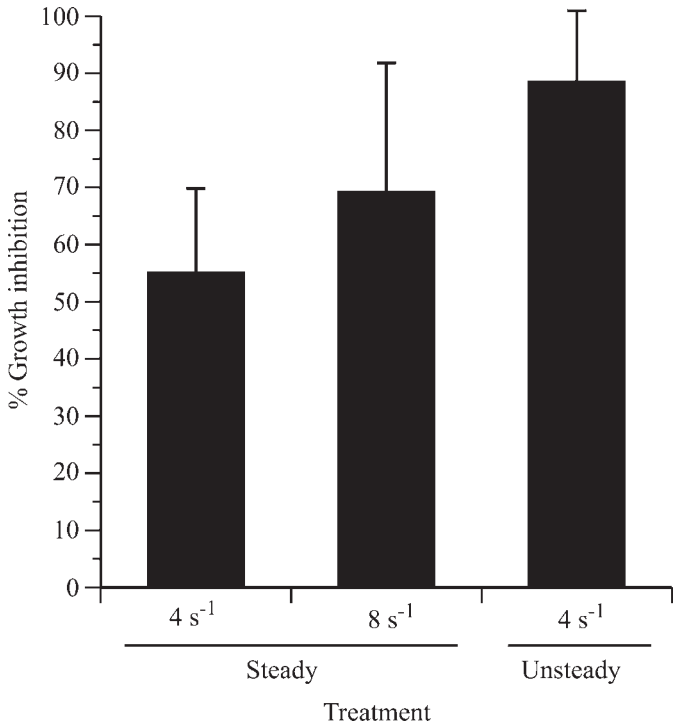

Fig. 4. Comparison of the effect of steady and unsteady flow on percentage inhibition of net population growth of *Lingulodinium polyedrum*, on the basis of the relative difference between net growth rates of still control and sheared cultures (*see* methods for details). Flow treatments included steady flow with average shears of 4 s^{-1} (expts. S2, S3) and 8 s^{-1} (expt. S4), and oscillatory flow with a period of 100 s (expts. O2–O4). Percentage growth inhibition is expressed as the mean ± SE. For the same average shear of 4 s^{-1}, unsteady flow resulted in a higher level of growth inhibition. Average growth inhibition for steady flow with an average shear of 8 s^{-1} was higher than that for steady flow with an average shear of 4 s^{-1} but less than that for the unsteady flow condition with an average shear of 4 s^{-1}.

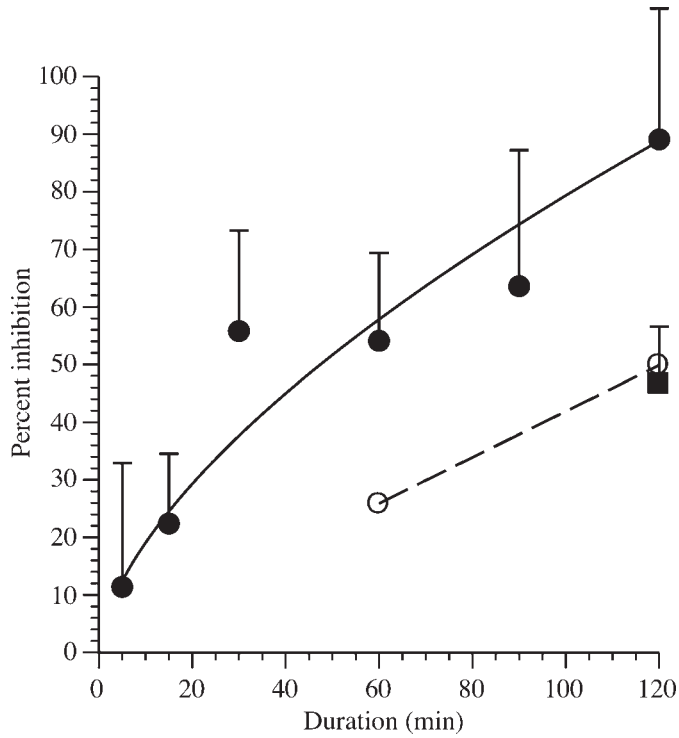

Fig. 5. Comparison of growth inhibition of *Lingulodinium polyedrum* as a function of the duration of steady and unsteady flow exposure. Unsteady flow treatments of varying durations (closed symbols) always had an average absolute shear of 4 s^{-1} and period of 100 s (expts. O10–O14); symbols represent the mean ± SE of four replicates per experiment. The solid line represents the least-squares power regression for the unsteady flow data, where $y = 4.58x^{0.620}$, $R^2 = 0.933$. Steady flow treatments had an average shear of 4 s^{-1} and include the pooled data of expts. S2 and S3 in the present study (solid box) and the data of Juhl and Latz (2002) (open circles) obtained using identical flow chambers. Growth inhibition increased with increasing flow duration, but unsteady flows always resulted in greater growth inhibition.

with a shear of 4 s^{-1} and the identical flow apparatus as in the present study, Juhl and Latz (2002) also found that growth inhibition of *L. polyedrum* increased with increasing duration of steady flow from 0–2 h. However, in this study the level of growth inhibition for a given shear duration and same absolute average shear was always higher for unsteady flow than for steady flow (Fig. 5).

Effect of maximum shear and average dissipation—Over a very limited parameter space that was not specifically designed for these comparisons, the relationship of growth inhibition from all experiments with 2 h d^{-1} shear duration (expts. S1–S7; O1–O9, O15, 16; R15, 16, Table 1) was explored as a function of maximum shear. Considering both steady and unsteady flow conditions, growth inhibition increased with maximum shear (Fig. 6A; $R^2 = 0.33$, $p < 0.001$). Although percentage growth inhibition was not correlated with maximum shear for unsteady flows with an average absolute value of 4 s^{-1} (expts. O1–O6; *t*-test, $t = -0.019$, df = 22, $p = 0.985$, $R^2 < 0.001$), the parameter space for unsteady flow was narrow, with maximum shear values varying less than twofold (6.4–11.3 s^{-1}).

A fundamental difference between steady and unsteady flow is that for unsteady flow the maximum shears are present for only a small fraction of the total flow exposure, whereas for steady flows the average and maximum shear levels are identical. Comparing between flow treatments with an identical maximum shear of 4 s^{-1}, growth inhibition of 45% ± 19% in unsteady flow (expts. O7–O9) was similar (*t*-test, $t = -0.125$, df = 16, $p = 0.902$) to that of 47% ± 27% for steady flows (expts. S2, S3).

As a function of the average kinetic energy dissipation per unit mass, ε, unsteady and steady flow at sufficiently high values of ε had dramatically different effects on growth inhibition (Fig. 6B). For low $\varepsilon \cong 10^{-6}$ m^2 s^{-3}, growth inhibition in steady and unsteady flows was similar. However, for $\varepsilon \geq 5 \times 10^{-6}$ m^2 s^{-3}, growth inhibition increased much more rapidly as a function of ε in unsteady flow compared with steady flow. Although more measurements are required before a definitive conclusion can be drawn, the implication of the present trends is that unsteady and steady flows with similar average rates of energy dissipation may result in dramatically different

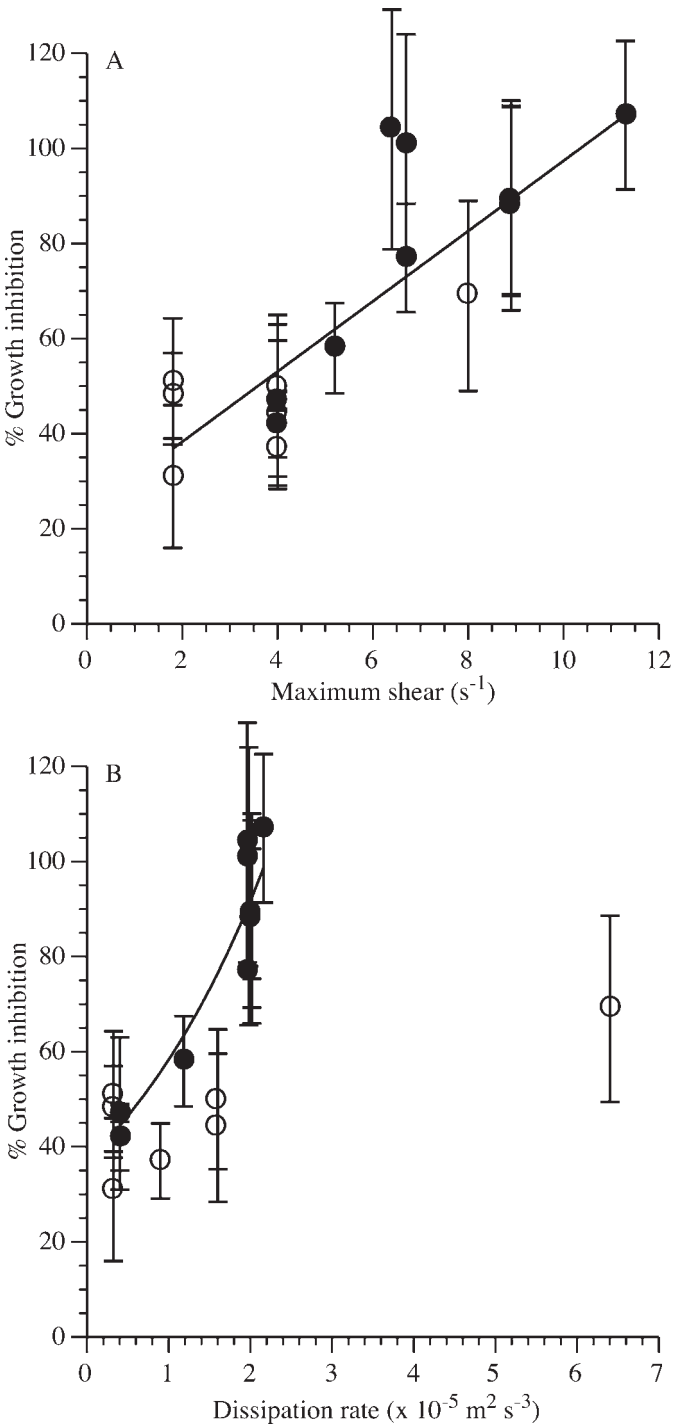

Fig. 6. Percentage inhibition of net population growth of *Lingulodinium polyedrum* as a function of maximum shear and dissipation rate of steady and unsteady flow exposure. Symbols represent average ± SE values of growth inhibition calculated from replicate experiments for steady (open symbols, expts. S1–S7) and unsteady (closed symbols, expts. O1–O9, O15, O16) flow treatments of 2 h d^{-1}. (A) Growth inhibition increased as a function of maximum shear. The line represents the least-squares linear regression for all data ($y = 7.4x + 24.9$, $R^2 = 0.331$, $p < 0.001$), indicating that percentage growth inhibition was significantly correlated with maximum shear. (B) Growth inhibition increased as a function of the dissipation rate. The line represents the least-squares exponential regression for unsteady flow ($y = 37.1e^{0.45x}$, $R^2 = 0.879$).

levels of growth inhibition. For $\varepsilon = 2 \times 10^{-5}$ m^2 s^{-3}, growth was completely inhibited in unsteady flow but only inhibited by about 50% in steady flow.

Experimental variability—Considering the variability in the net growth rates for the entire data set (Table 1), there was a significant difference in the standard deviations of still control (0.023 ± 0.011 d^{-1}, n =18) and all steady and unsteady flow (0.039 ± 0.014 d^{-1}, n = 25) experiments (t-test, $t = -4.200$, df = 41, $p < 0.001$). However, for the flow experiments there was no significant difference in the standard deviations for steady (0.034 ± 0.006 d^{-1}, n = 7) and unsteady (0.041 ± 0.016 d^{-1}, n = 18) flow (t-test, t = 1.129, df = 23, p = 0.271). Thus despite their lower net growth rates compared with still controls, there was greater variability in net growth rates for the flow treatments.

Discussion

Comparing growth response between steady and unsteady flow—The most important finding of this study is that unsteady flow can inherently have a more inhibitory effect on population growth than steady flow. Using a flow treatment with identical 2 h d^{-1} duration, predawn timing of exposure, and average absolute shear of 4 s^{-1} as in previous studies (Juhl et al. 2000; Juhl and Latz 2002), unsteady flows resulted in almost complete growth inhibition for the conditions tested, representing 50% more growth inhibition than that caused by steady flow with the same absolute average shear level. Because the maximum values of shear (expts. O5, O6) were higher than the steady shear case comparison (expts. S1, S2) with the same absolute average shear of 4 s^{-1}, a second series of experiments was conducted (expt. S4) using steady flow at a shear level higher than the previous maxima for unsteady flow. Although the unsteady flow treatments had maximum shears of 6.4 and 6.7 s^{-1} that were always less than the 8 s^{-1} steady flow treatment, nevertheless the unsteady experiments resulted in greater growth inhibition.

One explanation is that organisms underwent more rapid sensory adaptation to the steady 8 s^{-1} treatment such that the steady shear exposure resulted in a decrease in flow sensitivity compared with the unsteady flow condition. Adaptation is a common property of all sensory systems (Aidley 1998) and aids in enhancing the detection of changes in environmental conditions that are usually of more concern to an organism than steady conditions. The enhanced effect of unsteady flow on dinoflagellate growth inhibition compared with steady flow is consistent with a mechanism based on sensory adaptation. Dinoflagellates also exhibit sensory adaptation to changes in bioluminescence emission as a function of the rate of change of shear (von Dassow et al. 2005). It is important to understand how rate of change affects sensory adaptation to discriminate the effects of steady and unsteady flow on dinoflagellate physiology.

Treatments with lower average shear levels resulted in less growth inhibition and less difference between steady and unsteady flow conditions. Compared with steady flow with a shear level of 3.0 s^{-1}, which resulted in 36% growth

inhibition, unsteady flow with an average absolute shear of 3.1 s^{-1} resulted in greater growth inhibition of 60%. Repeating this comparison for an average and absolute shear of 1.8 s^{-1}, growth inhibition by unsteady and steady flows was similar. The shear threshold for growth inhibition by *L. polyedrum* for steady flow conditions has previously been reported as 2 s^{-1} where 17% growth inhibition occurred (Thomas and Gibson 1990*b*). The differences in shear thresholds and amount of growth inhibition between the Thomas and Gibson (1990*b*) study and the present study may be related to differences in methodology. The Thomas and Gibson (1990*b*) study used continuous illumination that resulted in net growth rates approximately double that in the present study; it is expected that flow-induced growth inhibition will be reduced under such conditions (Juhl et al. 2000). Furthermore, in the present study the flow treatment was given in the predawn hours when the organisms are most flow sensitive (Juhl et al. 2000; Juhl and Latz 2002), so greater growth inhibition is expected. The response threshold needs to be further explored for both unsteady and steady flows to understand how it varies with growth conditions. As all steady and unsteady flows are fully characterized in terms of the probability density function (pdf) of shear (e.g., Fig. 3C), growth inhibition can be explored in terms of the shear distribution. An index of integrated shear exposure can be determined from the shear pdf, after excluding shear levels that are less than the shear threshold for growth inhibition. Once an accurate shear threshold for growth inhibition is known, then the relationship between growth inhibition and integrated shear exposure can be further investigated.

Confirming previous results with steady flows (Juhl and Latz 2002), the amount of growth inhibition for both steady and unsteady flows was positively correlated with the daily duration of shear exposure from 0 to 2 h, with greater amounts of growth inhibition for unsteady flows than for steady flows with the same shear exposure time and average absolute shear of 4 s^{-1}. Because growth inhibition for average absolute shears greater than 1.8 s^{-1} was consistently greater in unsteady than steady flow conditions with the same average shear, the hypothesis is refuted.

Mechanisms of growth inhibition—Flow around cells can have both positive and negative effects on population growth. Flow enhances nutrient uptake by decreasing the thickness of the boundary layer surrounding an organism and enhancing mass transfer (Karp-Boss et al. 1996). This beneficial effect can be offset by negative effects, including a decrease in the rate of cell division that occurs in flows with low shears, and cell damage and mortality that occurs in flows with higher shears (Juhl and Latz 2002). Exposure of *L. polyedrum* to a steady shear of 4 s^{-1} inhibits growth primarily because of a decrease in the rate of cell division rather than an increase in mortality (Juhl and Latz 2002). In the present study using unsteady flow with an average absolute shear of 4 s^{-1}, the occasional observation of daughter cells in cultures with dead cells suggests that changes in both the rate of cell division and, to a lesser extent, in the mortality rate may be occurring. Detailed study of the contributions of division and mortality via flow cytometry is needed to quantitatively assess the competing mechanisms leading to changes in net growth under different flow.

The growth of dinoflagellates (Smith and Muscatine 1999; Van Dolah and Leighfield 1999) and other phytoplankton (Vaulot 1995) is regulated by the duration of the G_1 phase of the cell cycle. Dinoflagellate growth inhibition due to mechanical stress or flow appears to occur via cell cycle arrest at a G_1 checkpoint (Juhl and Latz 2002; Yeung and Wong 2003), as found in mammalian cells responding to flow (Akimoto et al. 2000). The resulting decrease in division rate may be an adaptive mechanism to reduce mechanical damage to the genome, which contains up to 20 times more deoxyribonucleic acid than most other eukaryotic cells (Holm-Hansen 1969). Cell strain caused by fluid shear may impart forces on the nucleus (Lynch and Lintilhac 1997), risking damage to the mitotic spindle or chromosomes during mitosis. Maximum flow sensitivity for *L. polyedrum* growth inhibition occurs near dawn (Juhl et al. 2000), coinciding with the time of mitosis (Juhl and Latz 2002) when cells are undergoing cytoskeletal rearrangement involving movement of the chromosomes.

The process whereby dinoflagellates transduce a mechanical stimulus to an intracellular biochemical signal is completely unknown. One possible mechanism involves flow interaction with membrane-associated proteins, in which the mechanical energy of the flow alters the membrane biophysical properties to activate a signal transduction pathway. In support of this mechanism, the fluidity of the plasma membrane of *L. polyedrum* is altered by flow (Mallipattu et al. 2002), and high levels of shear appear to activate guanosine-5′-triphosphate-binding proteins (Chen et al. 2007) that initiate a signaling pathway for dinoflagellate bioluminescence involving an increase in cytoplasmic [Ca^{2+}] (von Dassow and Latz 2002). An alterative mechanism is that the fluid force is transmitted through the cytoskeleton to act on intracellular receptors within the nucleus that inhibit cyclin-dependent kinases, which regulate the progression of cells through cell cycle checkpoints and are present in eukaryotic cells including dinoflagellates (Rodriguez et al. 1993; Van Dolah and Leighfield 1999). Inhibition of cyclin-dependent kinases is the mechanism by which the growth of mammalian endothelial cells is inhibited by blood flow (Akimoto et al. 2000). It is unknown which of these proposed mechanisms would be more sensitive to unsteady flow, but such knowledge would provide insight into the transduction process and signaling pathway(s) involved in flow sensing and growth inhibition.

A more general mechanism for growth inhibition is that force transmission throughout the cell induces cellular damage that involves a metabolic cost to repair. There is no conclusive evidence that the low levels of shear stress involved in this study, of the order of 10^{-3} to 10^{-2} N m^{-2}, can damage cells, although the presence of occasional dead cells suggests a source of mortality that requires additional investigation. The shear threshold for *L. polyedrum* bioluminescence is about two orders of magnitude greater

than for inhibition of population growth (Latz et al. 1994; Latz and Rohr 1999), consistent with its antipredation function (Morin 1983). Thus dinoflagellates can experience relatively high levels of shear without damage, although the time course of exposure needs to be considered. Evidence for oxidative stress in sheared cultures of *L. polyedrum* (Juhl and Latz 2002) suggests that mortality may originate from a biochemical process rather than mechanical damage. In mammalian endothelial cells, shear exposure induces the production of reactive oxygen species (Howard et al. 1997) implicated in the progression of cardiovascular disease.

Comparison with effects of unsteady flow in other cell types—The present study applied an approach similar to that used in investigating the response of mammalian endothelial cells to unsteady arterial blood flow. The endothelium experiences pulsatile flow, while regions of flow separation and recirculation have flow patterns that are oscillatory with changing flow direction (Barakat and Lieu 2003). Like the initial studies investigating flow-induced growth inhibition in dinoflagellates and other planktonic organisms, the effects of blood flow on the endothelium were initially studied using steady shear conditions to understand the mechanisms of flow sensing and response (Gudi et al. 1996; Malek and Izumo 1996). It is now recognized that the endothelium responds differently to steady and unsteady (oscillatory or pulsatile) laminar flow in terms of morphology, growth, oxidative stress, and gene expression (Barakat and Lieu 2003; Yee et al. 2008). The experimental approach used in this study can be applied for further study of the effect of fully characterized flow conditions on dinoflagellates and other planktonic organisms.

Comparison with previous studies of flow-stimulated inhibition of dinoflagellate growth—Because of the inherent variability associated with growth experiments, it was anticipated that the present experiments, which compare growth under different flow conditions, would be associated with a relatively large degree of uncertainty. To address this issue, the experimental plan entailed within-experiment replication consisting of four simultaneous replicate chambers per shear treatment and four simultaneous still control chambers. This amount of replication is more than that typical in growth studies involving turbulent flows (Thomas and Gibson 1990*a*; Dolan et al. 2003; Sullivan and Swift 2003). Furthermore, the chosen parameter space allowed direct comparison with the results of previous steady shear studies using similar apparatus and protocols, including illumination level, culture medium, and strain of *L. polyedrum* (Juhl et al. 2000; Juhl and Latz 2002).

Making this comparison, the range of still control growth rates of 0.10–0.19 d^{-1} in the present study was similar to the range of 0.12–0.20 d^{-1} for the previous studies (Juhl et al. 2000; Juhl and Latz 2002). Moreover, for steady flow with a shear of 4 s^{-1} and 2 h d^{-1} duration, the 47% growth inhibition obtained in the present study was similar to the 50% growth inhibition obtained by Juhl and Latz (2002) for the identical flow condition.

Net growth reflects conditions such as illumination level and duration, growth medium, temperature, and strain differences in growth phenotype. A confounding problem in comparing different population growth studies is the use of different experimental conditions, such as illumination and growth phase (Juhl et al. 2000; Juhl and Latz 2002). For *L. polyedrum*, the amount of growth inhibition due to steady flow is related to the net growth rate for the corresponding still controls; experimental treatments yielding higher net growth rates in the still controls resulted in less flow-induced growth inhibition (Juhl et al. 2000). In a previous study using steady Couette flow (Thomas and Gibson 1990*a*), net growth rates in the still controls were more than double that in the present study. As expected, steady flow with a shear of 2 s^{-1}, near the shear threshold, resulted in less growth inhibition (17%) for Thomas and Gibson (1990*a*) than that obtained in the present study (44%) for a similar constant shear level. However, a higher shear of 4 s^{-1} resulted in greater (75%) growth inhibition for Thomas and Gibson (1990*a*) than other studies (47–50%: Juhl et al. 2000; Juhl and Latz 2002; present study) for identical shear conditions but with a different Couette flow chamber configuration and suite of growth conditions.

Comparisons are even more complicated when relating studies using different types of unsteady flow. For example, in the turbulent flow study of Sullivan et al. (2003), in which the growth rates of still controls of *L. polyedrum* were more than double that in the present study, turbulent flow with $\varepsilon = 2 \times 10^{-5}\ m^2\ s^{-3}$, similar to that in the present study, enhanced population growth by 34% compared with complete inhibition of growth in this study. At $\varepsilon \sim 10^{-4}\ m^2\ s^{-3}$, equivalent to an average absolute shear of 10 s^{-1}, growth was enhanced by 37–61% (Sullivan and Swift 2003; Sullivan et al. 2003), whereas steady flow with the same average shear level inhibited growth by 45% (Juhl and Latz 2002). Only at the highest turbulence treatment was there growth inhibition (Sullivan et al. 2003), with variability similar to that in this study. The differences among studies can be attributable to the use of different dinoflagellate strains and growth conditions, as well as the flow conditions, which differ in the duration of exposure, flow intermittency, and time of day of exposure. Couette flow treatments are restricted to the time of day of maximum flow sensitivity and subject every organism to a similar shear exposure (Juhl et al. 2000; Juhl and Latz 2002; present study); turbulence treatments are integrated among times when organisms are less sensitive, and spatial heterogeneity of turbulence within the test chambers may offer a refuge from flow exposure. Until the relative effects of differences in hydrodynamics, growth conditions, and strain sensitivity can be assessed, any comparison of results obtained with different experimental conditions should be made with caution.

Relevance to oceanic conditions—The objective of this study was not to recreate turbulent oceanic flow conditions in the laboratory, but to establish a robust experimental system for comparing the effects of steady and unsteady flows on dinoflagellate growth. The use of experimental chambers identical to those used in previous studies

involving steady flow, while allowing a direct comparison to previous results, also limited the timescales of oscillation that provided a similar shear history everywhere in the 0.7-cm chamber gap. Oscillation periods <60 s did not provide similar shear histories throughout the flow chamber so they were not considered in this study.

Eddies and gyres spun off from the major currents have timescales of weeks or months, and as energy cascades through smaller and smaller scales of turbulence, the characteristic time for rotation decreases to seconds at the smallest scales (Mann and Lazier 1991). However, a 60-s period is of the same order of magnitude as the turbulent timescales within a turbulent oceanic boundary layer, for a 7-m wind speed and a depth of 7 m (Jones and Toba 2001).

Average levels of kinetic energy dissipation per unit mass in the present experiments were of the order of 10^{-5} to 10^{-6} m^2 s^{-3}, comparable with levels found in the upper parts of the oceanic mixed layer (Shay and Gregg 1984; Gargett 1989), although higher values can occur during more vigorous wind or wave forcing (Soloviev et al. 1988; Agrawal et al. 1992; Terray et al. 1996). However, the Kolmogorov timescale, $(\nu/\varepsilon)^{1/2}$, associated with these levels of oceanic dissipation is calculated to be 0.3–1 s, much less than the oscillation times achieved in this study.

Future work with smaller gap chambers and oscillation periods would allow for better emulation of the timescales of unsteady flow used in grid turbulence studies; a disadvantage is that the smaller test volumes may make growth experiments more difficult. Regardless, the significant effect on dinoflagellate growth as related to the steady or unsteady nature of the flow has serious implications on whether we can reliably compare steady and unsteady flows at any timescale. Furthermore, the timescale of turbulent velocity fluctuations needs to be considered in context with the timescale of organism response and sensory integration, which is unknown for growth inhibition.

In summary, these results demonstrate that different experimental approaches involving steady and unsteady flows with the same value of average absolute shear or average dissipation rate can result in significantly different levels of population growth. Consequently, comparing results from experimental studies using different flow fields that are characterized only in average flow terms must be approached with caution. Approaches that allow full analytical or numerical characterization of the flow conditions provide a framework for detailed investigations into the flow dynamics that affect aquatic organisms.

If growth inhibition is related to the unsteady nature of the flow or the distribution of shear values during flow exposure, analyses on the basis of average flow values will be insufficient. These implications are relevant not only to dinoflagellate growth but also for the effects of flow on plankton competition, predation, and behavior (Kiørboe and Saiz 1995; Welch et al. 1999; Stiansen and Sundby 2001). Through the use of computer-controlled flow systems, sophisticated shear waveforms that approximate in vivo arterial circulation are now being applied to the study of mammalian endothelial cells (Dai et al. 2004; Yee et al. 2006). In the same way, the present study using fully characterized steady, oscillatory, and rectified flows is but a first step toward understanding how unsteady flow affects dinoflagellate physiology. Treatments considering an expanded parameter space and more complex shear waveforms can more closely approximate the conditions present in oceanic turbulent flow, and further investigate the effect of fully characterized unsteady flow on phytoplankton growth and physiology.

Acknowledgments

We thank G. Anderson for fabrication of the flow apparatus and software development, V. Mandyam and E. Mercado for assistance with initial experiments, J. Crocket for additional calculations, T. Cowles, G. Deane, P. Franks, A. Juhl, K. Melville, and R. Pinkel for helpful discussions, and an anonymous reviewer for useful comments on the manuscript.

This research was partially supported by the Independent Applied Research Program funds to J.R. through the Space and Warfare Systems Center Pacific at San Diego. E. Mercado was supported by the Summer Training Academy for Research in the Sciences (STARS) at the University of California San Diego.

References

Agrawal, Y. C., and others. 1992. Enhanced dissipation of kinetic energy beneath surface waves. Nature **359:** 219–220.

Aidley, D. J. 1998. The physiology of excitable cells, 4th ed. Cambridge Univ. Press.

Akimoto, S., M. Mitsumata, T. Sasaguri, and Y. Yoshida. 2000. Laminar shear stress inhibits vascular endothelial cell proliferation by inducing cyclin-dependent kinase inhibitor p21*Sdi1/Cip1/Waf1*. Circ. Res. **86:** 185–190.

Alcaraz, M., E. Saiz, C. Marrase, and D. Vaque. 1988. Effects of turbulence on the development of phytoplankton biomass and copepod populations in marine microcosms. Mar. Ecol. Prog. Ser. **49:** 117–125.

Allen, W. E. 1946. "Red water" in La Jolla Bay in 1945. Trans. Am. Microsc. Soc. **65:** 149–153.

Anis, A., and J. N. Moum. 1995. Surface wave-turbulence interactions—scaling epsilon(Z) near the sea surface. J. Phys. Oceanogr. **25:** 2025–2045.

Barakat, A. I., and D. K. Lieu. 2003. Differential responsiveness of vascular endothelial cells to different types of fluid mechanical shear stress. Cell Biochem. Biophys. **38:** 323–343.

Berdalet, E., F. Peters, V. L. Koumandou, C. Roldan, O. Guadayol, and M. Estrada. 2007. Species-specific physiological response of dinoflagellates to quantified small-scale turbulence. J. Phycol. **43:** 965–977.

Berman, T., and B. Shteinman. 1998. Phytoplankton development and turbulent mixing in Lake Kinneret (1992–1996). J. Plankton Res. **20:** 709–726.

Bolli, L., G. Llaveria, E. Garces, O. Guadayol, K. Van Lenning, F. Peters, and E. Berdalet. 2007. Modulation of ecdysal cyst and toxin dynamics of two *Alexandrium* (Dinophyceae) species under small-scale turbulence. Biogeosciences **4:** 559–567.

Brainerd, K. E., and M. C. Gregg. 1993. Diurnal restratification and turbulence in the oceanic surface mixed-layer. 1. Observations. J. Geophys. Res. Oceans **98:** 22645–22656.

Chen, A. K., M. I. Latz, P. Sobolewski, and J. A. Frangos. 2007. Evidence for the role of G-proteins in flow stimulation of dinoflagellate bioluminescence. Am. J. Physiol. Regul. Integr. Comp. Physiol. **292:** R2020–R2027.

Dai, G. H., and others. 2004. Distinct endothelial phenotypes evoked by arterial waveforms derived from atherosclerosis-susceptible and -resistant regions of human vasculature. Proc. Natl. Acad. Sci. USA **101:** 14871–14876.

Dardik, A., L. Chen, J. Frattini, H. Asada, F. Aziz, F. A. Kudo, and B. E. Sumpio. 2005. Differential effects of orbital and laminar shear stress on endothelial cells. J. Vasc. Surg. **41:** 869.

Dolan, J. R., N. Sall, A. Metcalfe, and B. Gasser. 2003. Effects of turbulence on the feeding and growth of a marine oligotrich ciliate. Aquat. Microb. Ecol. **31:** 183–192.

Drennan, W. M., M. A. Donelan, E. A. Terray, and K. B. Katsaros. 1996. Oceanic turbulence dissipation measurements in SWADE. J. Phys. Oceanogr. **26:** 808–815.

Fox, R. W., A. T. McDonald, and P. J. Pritchard. 2004. Introduction to fluid mechanics, 6th ed. John Wiley & Sons.

Gargett, A. E. 1989. Ocean turbulence. Annu. Rev. Fluid Mech. **21:** 419–451.

Gudi, S. R. P., C. B. Clark, and J. A. Frangos. 1996. Fluid flow rapidly activates G proteins in human endothelial cells. Involvement of G proteins in mechanochemical signal transduction. Circ. Res. **79:** 834–839.

Guillard, R. R. L., and J. H. Ryther. 1962. Studies of marine planktonic diatoms. I. *Cyclotella nana* Hustedt, and *Detonula confervacea* (Cleve) Gran. Can. J. Microbiol. **8:** 229–239.

Harrison, W. G. 1976. Nitrate metabolism of the red tide dinoflagellate *Gonyaulax polyedra* Stein. J. Exp. Mar. Biol. Ecol. **21:** 199–209.

Havskum, H., P. J. Hansen, and E. Berdalet. 2005. Effect of turbulence on sedimentation and net population growth of the dinoflagellate *Ceratium tripos* and interactions with its predator, *Fragilidium subglobosum*. Limnol. Oceanogr. **50:** 1543–1551.

Hinze, J. O. 1975. Turbulence. McGraw-Hill.

Holm-Hansen, O. 1969. Algae amounts of DNA and organic carbon in single cells. Science **163:** 87–88.

Howard, A. B., R. W. Alexander, R. M. Nerem, K. K. Griendling, and W. R. Taylor. 1997. Cyclic strain induces an oxidative stress in endothelial cells. Am. J. Physiol. **272:** C421–C427.

Jones, I. S. F. and Y. Toba [Eds.]. 2001. Wind stress over the ocean. Cambridge Univ. Press.

Juhl, A. R., and M. I. Latz. 2002. Mechanisms of fluid shear-induced inhibition of population growth in a red-tide dinoflagellate. J. Phycol. **38:** 683–694.

———, V. L. Trainer, and M. I. Latz. 2001. Effect of fluid shear and irradiance on population growth and cellular toxin content of the dinoflagellate *Alexandrium fundyense*. Limnol. Oceanogr. **46:** 758–764.

———, V. Velazquez, and M. I. Latz. 2000. Effect of growth conditions on flow-induced inhibition of population growth of a red-tide dinoflagellate. Limnol. Oceanogr. **45:** 905–915.

Karp-Boss, L., E. Boss, and P. A. Jumars. 1996. Nutrient fluxes to planktonic osmotrophs in the presence of fluid motion. Oceanogr. Mar. Biol. Ann. Rev. **34:** 71–107.

Kiørboe, T. 1993. Turbulence, phytoplankton cell size, and the structure of pelagic food webs. Adv. Mar. Biol. **29:** 1–72.

———, and E. Saiz. 1995. Planktivorous feeding in calm and turbulent environments, with emphasis on copepods. Mar. Ecol. Prog. Ser. **122:** 135–145.

Latz, M. I., J. F. Case, and R. L. Gran. 1994. Excitation of bioluminescence by laminar fluid shear associated with simple Couette flow. Limnol. Oceanogr. **39:** 1424–1439.

———, and J. Rohr. 1999. Luminescent response of the red tide dinoflagellate *Lingulodinium polyedrum* to laminar and turbulent flow. Limnol. Oceanogr. **44:** 1423–1435.

Lazier, J. R. N., and K. H. Mann. 1989. Turbulence and the diffusive layers around small organisms. Deep-Sea Res. **36:** 1721–1733.

Lynch, T. M., and P. M. Lintilhac. 1997. Mechanical signals in plant development: A new method for single cell studies. Dev. Biol. **181:** 246–256.

Mackenzie, B. R., and W. C. Leggett. 1993. Wind-based models for estimating the dissipation rates of turbulent energy in aquatic environments—empirical comparisons. Mar. Ecol. Prog. Ser. **94:** 207–216.

Malek, A. M., and S. Izumo. 1996. Mechanism of endothelial cell shape change and cytoskeletal remodeling in response to fluid shear stress. J. Cell Sci. **109:** 713–726.

Malits, A., F. Peters, M. Bayer-Giraldi, C. Marrase, A. Zoppini, O. Guadayol, and M. Alcaraz. 2004. Effects of small-scale turbulence on bacteria: A matter of size. Microb. Ecol. **48:** 287–299.

Mallipattu, S. K., M. A. Haidekker, P. von Dassow, M. I. Latz, and J. A. Frangos. 2002. Evidence for shear-induced increase in membrane fluidity in the dinoflagellate *Lingulodinium polyedrum*. J. Comp. Physiol. A **188:** 409–416.

Mann, K. H., and J. R. N. Lazier. 1991. Dynamics of marine ecosytems. Blackwell Scientific Publications.

Margalef, R. 1997. Turbulence and marine life. Sci. Mar. **61:** 109–123.

———, M. Estrada, and D. Blasco. 1979. Functional morphology of organisms involved in red tides, as adapted to decaying turbulence, p. 89–94. *In* D. Taylor and H. Seliger [eds.], Toxic dinoflagellate blooms. Elsevier.

Morin, J. G. 1983. Coastal bioluminescence: Patterns and functions. Bull. Mar. Sci. **33:** 787–817.

Panton, R. 1968. The transient for Stokes's oscillating plate: A solution in terms of tabulated functions. J. Fluid Mech. **31:** 819–825.

Peters, F., and T. Gross. 1994. Increased grazing rates of microplankton in response to small-scale turbulence. Mar. Ecol. Prog. Ser. **115:** 299–307.

———, C. Marrase, H. Havskum, F. Rassoulzadegan, J. Dolan, M. Alcaraz, and J. M. Gasol. 2002. Turbulence and the microbial food web: Effects on bacterial losses to predation and on community structure. J. Plankton Res. **24:** 321–331.

———, and J. M. Redondo. 1997. Turbulence generation and measurement: Application to studies on plankton. Sci. Mar. **61:** 205–228.

Pollingher, U., and E. Zemel. 1981. *In situ* and experimental evidence of the influence of turbulence on cell division processes of *Peridinium cinctum* forma *westii* (Lemm.) Lefèvre. Br. Phycol. J. **16:** 281–287.

Rodriguez, M., J. W. Cho, H. W. Sauer, and P. J. Rizzo. 1993. Evidence for the presence of a cdc2-like protein kinase in the dinoflagellate *Crypthecodinium cohnii*. J. Eukaryot. Microbiol. **40:** 91–96.

Rohr, J., M. Hyman, S. Fallon, and M. I. Latz. 2002. Bioluminescence flow visualization in the ocean: An initial strategy based on laboratory experiments. Deep-Sea Res. I **49:** 2009–2033.

Schlichting, H. 1979. Boundary-layer theory. McGraw-Hill.

Shay, T. J., and M. C. Gregg. 1984. Turbulence in an oceanic convective mixed layer. Nature **310:** 282–285.

Smayda, T. J. 2000. Ecological features of harmful algal blooms in coastal upwelling ecosystems. S. Afr. J. Mar. Sci. **22:** 219–253.

———, and C. S. Reynolds. 2001. Community assembly in marine phytoplankton: Application of recent models to harmful dinoflagellate blooms. J. Plankton Res. **23:** 447–461.

Smith, G. J., and L. Muscatine. 1999. Cell cycle of symbiotic dinoflagellates: Variation in G1 phase-duration with anemone nutritional status and macronutrient supply in the *Aiptasia pulchella–Symbiodinium pulchrorum* symbiosis. Mar. Biol. **134:** 405–418.

Smyth, W. D., and J. N. Moum. 2001. 3D turbulence. Encyclopedia of ocean sciences. Academic Press.

Soloviev, A. V., N. V. Vershinsky, and V. A. Bezverchnii. 1988. Small-scale turbulence measurements in the thin surface layer of the ocean. Deep-Sea Res. **35:** 1859–1874.

Stiansen, J. E., and S. Sundby. 2001. Improved methods for generating and estimating turbulence in tanks suitable for fish larvae experiments. Sci. Mar. **65:** 151–167.

Stoecker, D. K., A. Long, S. E. Suttles, and L. P. Sanford. 2006. Effect of small-scale shear on grazing and growth of the dinoflagellate *Pfiesteria piscicida*. Harmful Algae **5:** 407–418.

Sullivan, J. M., and E. Swift. 2003. Effects of small-scale turbulence on net growth rate and size of ten species of marine dinoflagellates. J. Phycol. **39:** 83–94.

———, E. Swift, P. L. Donaghay, and J. E. B. Rines. 2003. Small-scale turbulence affects the division rate and morphology of two red-tide dinoflagellates. Harmful Algae **2:** 183–199.

Sweeney, B. M. 1975. Red tides I have known, p. 225–234. *In* V. R. LoCicero [ed.], Proc. First Intl. Conf. Toxic Dinoflagellates. The Massachusetts Science and Technology Foundation.

Taylor, G. I. 1923. Stability of a viscous liquid contained between two rotating cylinders. Phil. Trans. Roy. Soc. Lond. **223:** 289–343.

Tennekes, H., and J. L. Lumley. 1972. A first course in turbulence. MIT Press.

Terray, E. A., and others. 1996. Estimates of kinetic energy dissipation under breaking waves. J. Phys. Oceanogr. **26:** 792–807.

Thomas, W. H., and C. H. Gibson. 1990*a*. Effects of small-scale turbulence on microalgae. J. Appl. Phycology **2:** 71–77.

———, and ———. 1990*b*. Quantified small-scale turbulence inhibits a red tide dinoflagellate, *Gonyaulax polyedra* Stein. Deep-Sea Res. **37:** 1583–1593.

Van Dolah, F. M., and T. A. Leighfield. 1999. Diel phasing of the cell-cycle in the Florida red tide dinoflagellate, *Gymnodinium breve*. J. Phycol. **35:** 1404–1411.

Van Duuren, F. A. 1968. Defined velocity gradient model flocculator. Proc. Am. Soc. Civ. Engr. **94:** 671–682.

Vaulot, D. 1995. The cell cycle of phytoplankton: Coupling cell growth to population growth. NATO ASI Ser. Ser. G Ecol. Sci. **38:** 303–322.

Veron, F., and W. K. Melville. 1999. Pulse-to-pulse coherent Doppler measurements of waves and turbulence. J. Atmos. Ocean. Technol. **16:** 1580–1597.

von Dassow, P., R. N. Bearon, and M. I. Latz. 2005. Bioluminescent response of the dinoflagellate *Lingulodinium polyedrum* to developing flow: Tuning of sensitivity and the role of desensitization in controlling a defensive behavior of a planktonic cell. Limnol. Oceanogr. **50:** 607–619.

———, and M. I. Latz. 2002. The role of Ca^{2+} in stimulated bioluminescence of the dinoflagellate *Lingulodinium polyedrum*. J. Exp. Biol. **205:** 2971–2986.

Welch, J. M., R. B. Forward, and P. A. Howd. 1999. Behavioral responses of blue crab *Callinectes sapidus* postlarvae to turbulence: Implications for selective tidal stream transport. Mar. Ecol. Prog. Ser. **179:** 135–143.

White, A. W. 1976. Growth inhibition caused by turbulence in the toxic marine dinoflagellate *Gonyaulax excavata*. J. Fish. Res. Bd. Canada **33:** 2598–2602.

Yee, A., K. A. Bosworth, D. E. Conway, S. G. Eskin, and L. V. McIntire. 2008. Gene expression of endothelial cells under pulsatile non-reversing vs. steady shear stress: Comparison of nitric oxide production. Ann. Biomed. Eng. **36:** 571–579.

———, Y. Sakurai, S. G. Eskin, and L. V. McIntire. 2006. A validated system for simulating common carotid arterial flow in vitro: Alteration of endothelial cell response. Ann. Biomed. Eng. **34:** 593–604.

Yeung, P. K. K., and J. T. Y. Wong. 2003. Inhibition of cell proliferation by mechanical agitation involves transient cell cycle arrest at G(1) phase in dinoflagellates. Protoplasma **220:** 173–178.

Zar, J. H. 1974. Biostatistical analysis. Prentice-Hall.

Associate editor: Thomas Kiørboe

Received: 15 August 2008
Accepted: 16 February 2009
Amended: 17 March 2009